Diffusion in a Cu-Zr metallic glass studied by microsecond-scale molecular dynamics simulations

Y. Zhang, C. Z. Wang, M. I. Mendelev, F. Zhang, M. J. Kramer, and K. M. Ho

Phys. Rev. B **91**, 180201 — Published 5 May 2015

DOI: 10.1103/PhysRevB.91.180201

Diffusion in a Cu-Zr metallic glass studied by microsecond scale molecular dynamics simulations

Y. Zhang[1], C.Z. Wang[1,2,*], M.I. Mendelev[1], F. Zhang[1], M.J. Kramer [1,3] and K.M. Ho[1,2]

[1] *Ames Laboratory-USDOE, Iowa State University, Ames, Iowa 50011, USA*

[2] *Department of Physics and Astronomy, Iowa State University, Ames, Iowa 50011, USA*

[3] *Department of Materials Science and Engineering, Iowa State University, Ames, Iowa 50011, USA*

*wangcz@ameslab.gov

Abstract

Icosahedral short-range order (ISRO) has been widely accepted to be dominant in Cu-Zr metallic glasses (MGs). However, the diffusion mechanism and correlation of ISRO and medium-range order (MRO) to diffusion in MGs remain largely unexplored. In this work, we performed a long time annealing up to 1.8 μs in molecular dynamics (MD) simulations to study the diffusion mechanism and the relationship between atomic structures and diffusion path in a $Cu_{64.5}Zr_{35.5}$ MG. It is found that most of the diffusing events performed by the diffusing atoms are outside ISRO and the Bergman-type MRO (BMRO). The long-range diffusion in MGs is highly heterogeneous, via collective diffusing events through the liquid-like channels in the glass. Our results clearly demonstrate a strong correlation between the atomic structures and transport in MGs.

Metallic glasses [1] (MGs) are metastable materials. The metastability gives rise to various rearrangement processes at elevated temperatures [2,3], which calls for an understanding of the diffusion in MGs. Diffusion in metallic glasses is a highly collective processes [4], which is significantly different from diffusion in crystalline metals. Microscopically, diffusivity is closely related to the atomic mobility in MGs or supercooled liquids. A close relationship between atomic mobility and the local structure has been demonstrated in supercooled liquids [5]. However, the underlying influence of structure on atomic mobility is shown only local in time, fading out much shorter than the α-relaxation time [6]. Therefore many studies have been carried out focusing on a long time correlation, such as the dynamical facilitation which denotes propagation of the mobile regions due to the mobility transfer of mobile particles [7]. Molecular dynamics (MD) simulations of a supercooled $Ni_{0.5}Zr_{0.5}$ liquid with a time span of 1.0 μs has demonstrated marked correlations between atomic mobility and local structure parameters [8]. Regions of mobility change with time in the same system have also been revealed [9]. Recently, localized soft modes have been reported to have strong correlations to the atomic mobility and structures in Cu-Zr MGs [10].

However, in order to achieve a comprehensive understanding of the long-range diffusion in MGs, the diffusion path and its correlation to the atomic structures must be established. The difficulty for MD simulations lies in the following aspects: firstly, many MD simulations have revealed the coexistence of nanometer-sized liquid-like and solid-like regions in MGs [11,12]. The heterogeneous atomic structure can significantly impact the diffusion paths in MGs. Secondly, long-range diffusion in MGs is very hard to capture by MD simulations performed only at nanosecond timescale. Thirdly, the MGs produced by MD simulations are usually not well-relaxed due to the ultrahigh cooling rates.

Cu-Zr binary MG is a prototype of various Cu-Zr-based MGs [13-15], therefore the correlation between diffusion paths and atomic structures in Cu-Zr MG is the footstone to understanding diffusion in many Cu-Zr based metallic glasses. Structurally, icosahedral short-range order (ISRO) is widely accepted to be dominant [16,17], which is

responsible for low mobility in Cu-Zr supercooled liquids [18-20]. Vertex-, edge, face-sharing and interpenetrating icosahedra have been proposed as the medium range order (MRO) [21,22]. The Bergman type MRO (BMRO) has been revealed as another key MRO in $Cu_{64.5}Zr_{35.5}$ MGs by our group [23]. Recently, a sub-T_g annealing has been demonstrated to effectively reduce the effect of ultrahigh cooling rates used in MD simulations [24], which opens a door to investigate the long- range diffusion in well-relaxed MGs using MD simulations.

In this study, we adopted the $Cu_{64.5}Zr_{35.5}$ MG to study the long-range diffusion in well-relaxed MGs using MD simulations up to 1.8 μs. Such a long time interval enables a more reliable statistics of atomic structures and diffusion analysis than conventional MD simulations conducted at nanosecond timescale [25,26]. By analyzing the trajectories of the diffusing atoms, we found a strong correlation between the diffusion paths and atomic structures. The diffusing atoms strongly avoid the ISRO and BMRO during the course of MD simulation, while the liquid-like regions (depleted in ISRO or BMRO) can interconnect and form diffusion paths. Therefore the long-range diffusion in well-relaxed MGs does not take place uniformly in space, but is rather confined in the liquid-like regions.

Classical MD simulations of $Cu_{64.5}Zr_{35.5}$ MGs were performed using the Finnis-Sinclair type potential developed in Ref [27]. Despite being less accurate compared to *ab initio* methods, classical MD simulations enable the study of diffusion using a larger model size and a longer timescale. In addition, the adopted empirical potential has been demonstrated to capture many structural [28] and dynamical [18,29] features of $Cu_{64.5}Zr_{35.5}$ MGs or liquids observed by experiments or *ab initio* MD simulations. Isothermal-isobaric ensemble (*NPT*, N=5000 atoms, P=0) and Nosé-Hoover thermostat were used throughout the simulation. The time step for integration was 2.5 fs. After a pre-equilibration at 2000 K, the model was continuously quenched down to 700 K at 10^{10} K/s. Previous study has revealed the glass transition occurs around 750 K [23]. Therefore the as-quenched model is already in glassy state. The as-quenched model was annealed isothermally at 700 K for 1.8 μs. The atomic trajectory was recorded every 1 ns to study

the atomic structures and diffusion. The cluster alignment method [30] was adopted to characterize the atomic structure in terms of ISRO and BMRO. The self-diffusivity (D) is calculated using the Einstein's relation. Details of structural analysis and calculation of self-diffusivity can be found in supplemental materials [31].

The evolution of self-diffusivity during the long MD run is illustrated in Fig. 1(a). Several features can be observed here: (1) the Cu diffusivity is always about an order of magnitude larger than the Zr diffusivity. It is consistent with many studies, where smaller atoms were found to have larger diffusivity than the larger atoms in both metallic liquids and glasses [32]. (2), both Cu and Zr diffusivity decrease significantly within t=0-0.6 μs, whereas only a small diffusivity drop can be found from t=0.6 to 1.8 μs. At t=1.8 μs, the Cu diffusivity decreases by 7-8 times compared to the as-quenched state. (3), Frank [33] proposed that the experimental diffusivity can be described by $D(t)$-$D(0)$=[$D(t_f)$-$D(0)$]$exp(-1/\tau)$, where $D(t)$ is the instantaneous diffusivity, $D(0)$ and $D(t_f)$ are the diffusivity before and after the relaxation, respectively, and τ is the relaxation time. The diffusivity of the simulated $Cu_{64.5}Zr_{35.5}$ MGs can be well fitted with τ=38.8 and 41.2 ns for Cu and Zr, respectively, indicating that the long MD run has captured similar trend in experiments.

The time-dependent mean squared displacements (MSDs) are shown in Fig. 1(b). The MSDs of both Cu and Zr increase with time, indicating clearly a long-range diffusion behavior. Long-range diffusion in MGs has been found by experiments [34], whereas it is not readily accessible for MD simulation at nanosecond scale. The self-diffusivities of Cu at 700 K under various cooling rates without annealing were also measured and shown in Fig. 1(c). The self-diffusivity exhibits an overall trend to decrease exponentially with lower cooling rates. In the following we divide the whole MD run into two parts: (1) t=0-0.6 μs was used to achieve a well-relaxed glassy state and (2) t=0.6-1.8 μs was used to study the diffusion in Cu-Zr MGs.

We first set out to identify the diffusing atoms. Most of the studies on the dynamical heterogeneity or diffusion tried to monitor a certain fractions of mobile atoms

[35,36]. We adopt the same approach here. The diffusing atoms were selected according to their final displacement (d_f) at t=1.8 μs, using their positions at t=0.6 μs as reference. Here we use the cutoff d_f=1.7 nm, the population of the diffusing atoms selected in this way corresponds to 5% of the total atoms in the simulation box (see supplemental materials [31] for details). It should be pointed out that all the diffusing atoms identified under this scheme are Cu atoms.

Microscopically, the long-range diffusion in MGs is achieved by successive diffusing events. We define a diffusing event using both spatial and temporal metrics [37]: (1) the atom has to displace farther than a critical distance r_c=0.2 nm and (2) the atom has to pass r_c within 5ns (see supplemental materials [31] for details). Under this definition, we have identified 52,869 diffusing events performed by all the atoms during t=0.6-1.8 μs, among which 13,452 events performed by the diffusing atoms. Such a large number of events enable a reliable statistics. In the following we will focus on the diffusing events performed by the diffusing atoms. These events were classified according to the environments with respect to ISRO or BMRO before and after the event: (1) with respect to ISRO, there are three types of environments (ICO center, ICO neighbor and outside ICO). Hence there are nine types of events possible: e.g. events initiated outside ICO and ended at ICO center, ICO neighbor or remained outside ICO, etc. (2) with respect to BMRO, there are four types of environments (Bergman center, first shell, outer shell and outside Bergman). Thus 16 events types are possible. Nevertheless, the results shown in Fig. 2 (a) and (b) demonstrate that only several types of events are dominant. With respect to ISRO, 74.8% of the events take place outside the ICO. 10.3% of the events are from ICO neighbors to outside ICO. The events from outside ICO to ICO neighbors accounts for 10.8%. The possibility for events that initiate at ICO neighbor sites and end also at ICO neighbor is 3.3%. All the other types of events are negligible. Similar scenario is with respect to BMRO. 86.1% of the events occur outside the BMRO, which is the predominant type. 5.7% of the events are initiated at outer shells and ending outside the BMRO. The possibility for the reverse process, from outside to the outer shell of BMRO is almost equal (6.0%). Only 1.1% of the events occur within the outer shell. These results imply that diffusing atoms in $Cu_{64.5}Zr_{35.5}$ MGs

try to avoid ISRO and BMRO strongly. We also counted how long the diffusing atoms have been in ICO center, ICO neighbor or outside ICO, similarly in BMRO center, first shell, outer shells or outside BMRO during t=0.6-1.8 μs. As illustrated in Fig. 2 (c) and (d), diffusing atoms stay averagely for 0.897 and 0.957 μs outside ICO and BMRO, respectively, corresponding to 74.6% and 80.9% of the simulation time. In contrast, they spent only 0.9% and 0.8% of the simulation time at the center of ICO or BMRO. The diffusing atoms can also be detected at the ICO neighbor sites, first or outer shell of BMRO with the possibilities of 24.5%, 3.2% and 16.3%, respectively. These results clearly show that the diffusing atoms try to avoid the ISRO or BMRO for the majority of the simulation time.

Based on the above statistics, we further investigate the diffusion paths with respect to ISRO and BMRO in $Cu_{64.5}Zr_{35.5}$ MGs. Since the ISRO, BMRO and diffusing atoms undergo positional changes during the course of MD simulation, we use an isosurface to reflect the distribution density of ISRO and BMRO. Two isosurfaces were constructed: (1) all the atoms that have been involved in the ISRO or BMRO and (2) all the diffusion paths of the diffusing atoms (see supplemental materials [31] for details). It can be seen from Fig.3 that (1) the ISRO or BMRO aggregates to form a rigid network in Cu-Zr MGs and (2) the diffusion paths almost never overlap with ISRO or BMRO. Meanwhile, liquid-like regions (poor in ISRO or BMRO) can interconnect to form diffusion channels. It can be deduced that both the ISRO and BMRO networks will be much better developed in real Cu-Zr MGs (produced under even lower cooling rates) than the MD simulations. Therefore the liquid-like regions will be much smaller in size, resulting in the measured diffusivity to be several orders of magnitudes lower than the MD simulations [38].

We now investigate the diffusing paths by focusing on individual diffusing atoms. The distribution of final displacements of the diffusing atoms at t=1.8 μs is present in Fig. 4(a). The distribution follows an exponential decay. Some diffusing atoms can displace even as far as d_f=3.3 nm during t=0.6-1.8 μs. Here we select two diffusing atoms with the largest (3.3 nm) and smallest (1.7 nm) d_f to reveal the spatial correlation of their

trajectories to the ISRO and BMRO. The time-dependent displacements of these two diffusing atoms are shown in Fig. 4(b). Both diffusing atoms are very active during t=0.6-0.8 μs, as illustrated by a continuous increase in the displacement. During t=0.8-1.2 μs both diffusing atoms are sluggish, as reflected by the plateaus. However, the one with the largest d_f becomes active again during t=1.2-1.8 μs. These results demonstrate that diffusion in Cu-Zr MGs is composed of successive diffusing events in an intermittent nature, which is distinct from the diffusion in equilibrium metallic liquids (see supplemental materials [31] for details). The spatial correlations of the two trajectories to ISRO or BMRO are shown in Fig. 4(c-f). It can be clearly seen that the majority of the diffusion paths is located outside the ISRO and BMRO. Sometimes the diffusing atom will touch the boundary of the ISRO or BMRO, but they have very little chance to penetrate the ISRO and BMRO. We have further checked the diffusing events in the core of solid-like regions rich in ISRO. The trajectories of 20 atoms in the core of ISRO have been monitored at every MD step for 300 ns (see supplemental materials [31] for details), whereas no events of these atoms can be identified. It confirms that the atoms involved in the core of solid-like regions formed by ISRO have extremely low diffusivity. Lastly, we want to point out that all the correlations between the diffusion and the atomic structures are based on the behavior of Cu atoms. However, the diffusion mechanism of Zr atoms might be different.

In summary, we performed a long time sub-T_g annealing up to 1.8 μs achievable by MD simulations to investigate the correlation between atomic structures and diffusion paths in a Cu-Zr metallic glasses. Long-range diffusion is clearly observed during the MD simulations. We found that diffusing atoms in Cu-Zr MGs strongly avoid the icosahedral short range order and the Bergman-type medium range order. Meanwhile, the liquid-like regions can interconnect and form diffusion channels. Therefore the long range diffusion in Cu-Zr MGs does not take place uniformly, but is rather confined in the liquid like regions.

The research was performed at the Ames Laboratory, which is operated for the U.S. DOE by Iowa State University under contract # DE-AC02-07CH11358. The computer

time support came from National Energy Research Scientific Computing Center (NERSC) in Berkeley, CA.

References

[1] A. Inoue, Acta Mater. **48**, 279 (2000).
[2] H. S. Chen and E. Coleman, Appl. Phys. Lett. **28**, 245 (1976).
[3] Y. P. Mitrofanov, V. A. Khonik, A. V. Granato, D. M. Joncich, S. V. Khonik, and A. M. Khoviv, Appl. Phys. Lett. **100**, 171901 (2012).
[4] F. Faupel, W. Frank, M. P. Macht, H. Mehrer, V. Naundorf, K. Ratzke, H. R. Schober, S. K. Sharma, and H. Teichler, Rev. Mod. Phys. **75**, 237 (2003).
[5] A. Widmer-Cooper, P. Harrowell, and H. Fynewever, Phys. Rev. Lett **93**, 135701 (2004).
[6] G. A. Appignanesi, J. A. Rodríguez Fris, and M. A. Frechero, Phys. Rev. Lett **96**, 237803 (2006).
[7] J. Garrahan and D. Chandler, Phys. Rev. Lett **89**, 035704 (2002).
[8] I. Ladadwa and H. Teichler, Phys. Rev. E **73**, 031501 (2006).
[9] I. Ladadwa and H. Teichler, Phys. Rev. E **78**, 041503 (2008).
[10] Y. Zhang, C. Z. Wang, F. Zhang, M. I. Mendelev, M. J. Kramer, and K. M. Ho, Appl. Phys. Lett. **105**, 151910 (2014).
[11] T. Fujita, K. Konno, W. Zhang, V. Kumar, M. Matsuura, A. Inoue, T. Sakurai, and M. W. Chen, Phys. Rev. Lett **103**, 075502 (2009).
[12] M. Li, C. Z. Wang, S. G. Hao, M. J. Kramer, and K. M. Ho, Phys. Rev. B **80**, 184201 (2009).
[13] M. B. Tang, D. Q. Zhao, M. X. Pan, and W. H. Wang, Chinese Phys.Lett. **21**, 901 (2004).
[14] D. Wang, Y. Li, B. B. Sun, M. L. Sui, K. Lu, and E. Ma, Appl. Phys. Lett. **84**, 4029 (2004).
[15] D. Xu, B. Lohwongwatana, G. Duan, W. L. Johnson, and C. Garland, Acta Mater. **52**, 2621 (2004).
[16] G. Duan, D. H. Xu, Q. Zhang, G. Y. Zhang, T. Cagin, W. L. Johnson, and W. A. Goddard, Phys. Rev. B **71**, 224208 (2005).
[17] X. D. Wang, S. Yin, Q. P. Cao, J. Z. Jiang, H. Franz, and Z. H. Jin, Appl. Phys. Lett. **92**, 011902 (2008).
[18] S. G. Hao, C. Z. Wang, M. J. Kramer, and K. M. Ho, J. Appl. Phys. **107**, 053511 (2010).
[19] H. L. Peng, M. Z. Li, W. H. Wang, C. Z. Wang, and K. M. Ho, Appl. Phys. Lett. **96**, 021901 (2010).
[20] Y. Q. Cheng, H. W. Sheng, and E. Ma, Phys. Rev. B **78**, 014207 (2008).
[21] M. Lee, C.-M. Lee, K.-R. Lee, E. Ma, and J.-C. Lee, Acta Mater. **59**, 159 (2011).
[22] R. Soklaski, Z. Nussinov, Z. Markow, K. F. Kelton, and L. Yang, Phys. Rev. B **87**, 184203 (2013).
[23] X. W. Fang, C. Z. Wang, S. G. Hao, M. J. Kramer, Y. X. Yao, M. I. Mendelev, Z. J. Ding, R. E. Napolitano, and K. M. Ho, Sci. Rep. **1**, 194, 194 (2011).
[24] F. Zhang, M. I. Mendelev, Y. Zhang, C.-Z. Wang, M. J. Kramer, and K.-M. Ho, Appl. Phys. Lett. **104**, 061905 (2014).
[25] M. Kluge and H. R. Schober, Phys. Rev. B **70**, 224209, 224209 (2004).
[26] Y. L. Sun, J. Shen, and A. A. Valladares, J. Appl. Phys. **106**, 073520 (2009).
[27] M. I. Mendelev, M. J. Kramer, R. T. Ott, and D. J. Sordelet, Philos. Mag. **89**, 109 (2009).
[28] Y. Zhang, F. Zhang, C. Z. Wang, M. I. Mendelev, M. J. Kramer, and K. M. Ho, Phys. Rev. B **91**, 064105 (2015).
[29] L. Ward, D. Miracle, W. Windl, O. N. Senkov, and K. Flores, Phys. Rev. B **88**, 134205 (2013).
[30] X. W. Fang, C. Z. Wang, Y. X. Yao, Z. J. Ding, and K. M. Ho, Phys. Rev. B **82**, 184204 (2010).
[31] See Supplemental Material at [URL will be inserted by publisher] for details of structural analysis and calculation of self-diffusivity

[32] X. P. Tang, U. Geyer, R. Busch, W. L. Johnson, and Y. Wu, Nature **402**, 160 (1999).
[33] W. Frank, Defect Diffus. Forum **143**, 695 (1997).
[34] D. Gupta, K. N. Tu, and K. W. Asai, Phys. Rev. Lett **35**, 796 (1975).
[35] C. Donati, S. C. Glotzer, P. H. Poole, W. Kob, and S. J. Plimpton, Phys. Rev. E **60**, 3107 (1999).
[36] S. C. Glotzer, J. Non-cryst. Solids **274**, 342 (2000).
[37] K. Vollmayr-Lee, J. Chem. Phys. **121**, 4781 (2004).
[38] E. C. Stelter and D. Lazarus, Phys. Rev. B **36**, 9545 (1987).

Figures

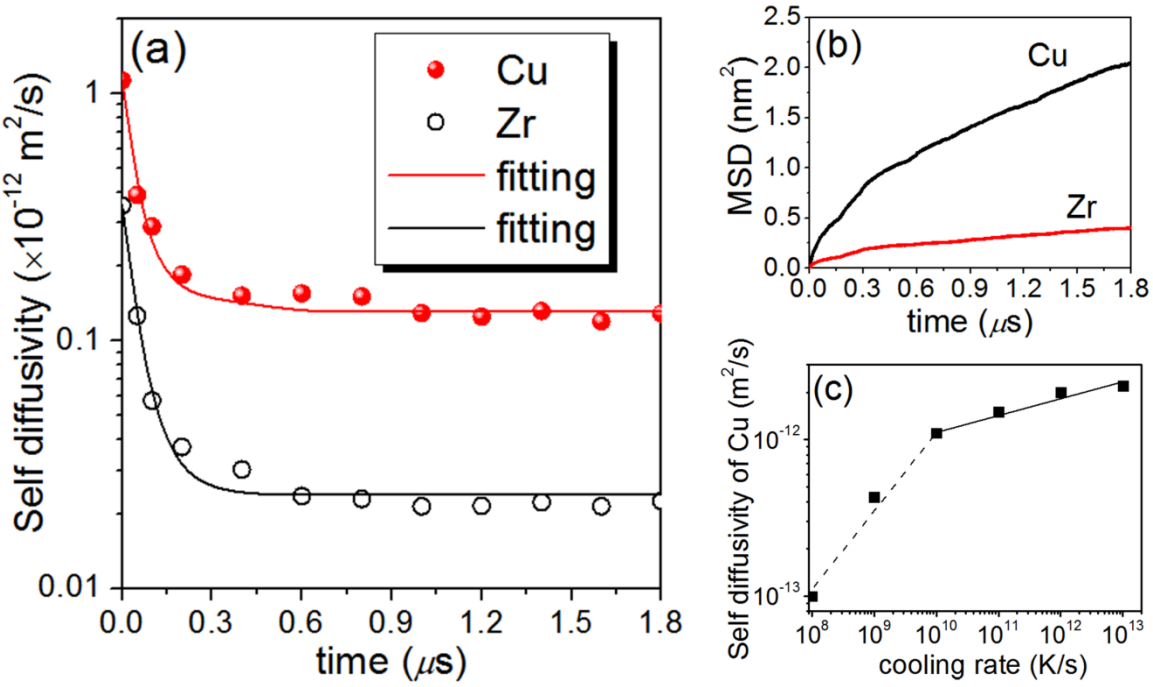

Fig. 1 (a) Self-diffusivity of Cu (full cycles) and Zr (open circles) atoms during MD simulation at 700 K. Solid lines indicate fitting using an exponential function. (b) The mean square displacements. (c) Cu Self-diffusivities at 700K as a function of cooling rates.

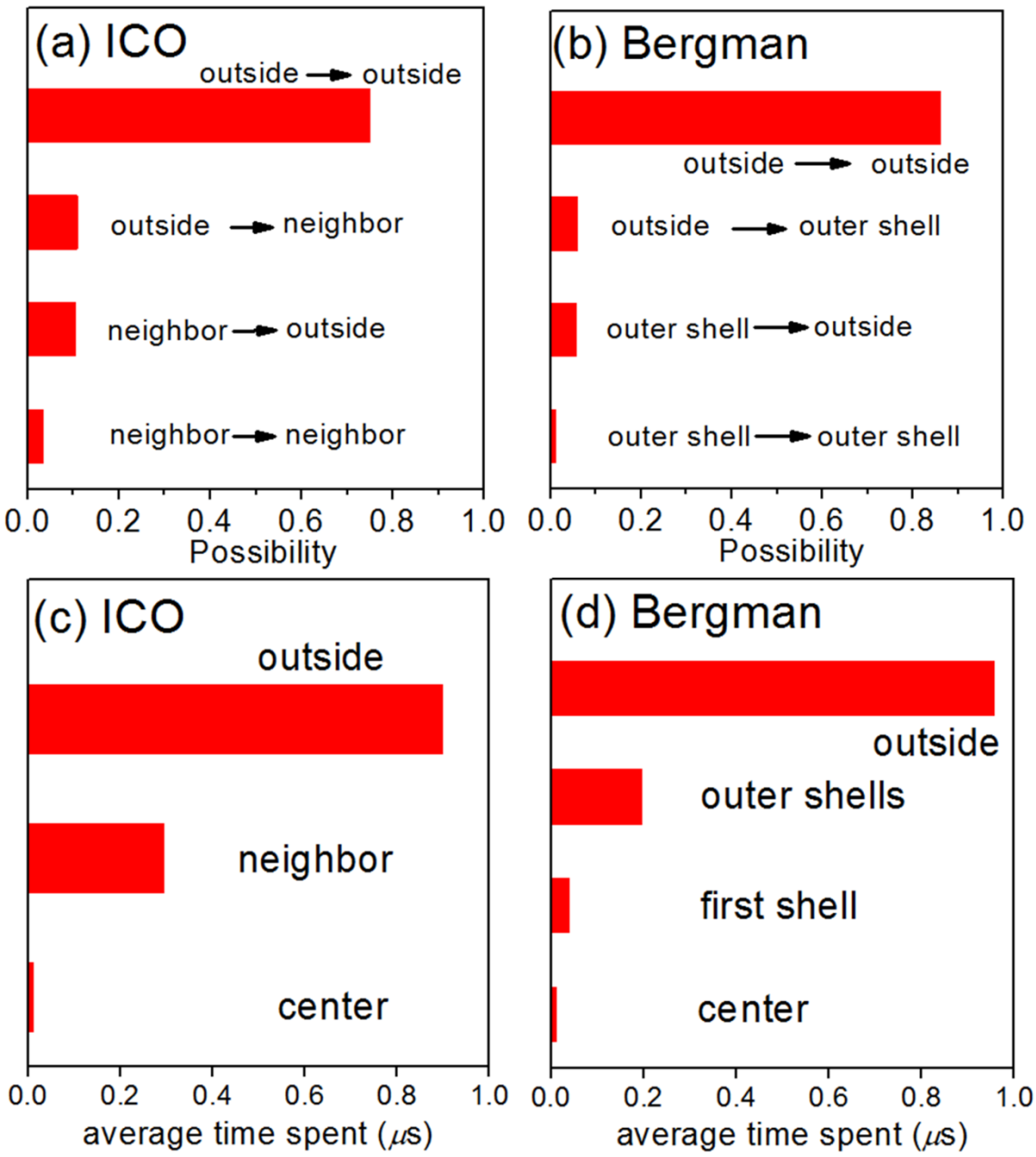

Fig. 2 Possibility of the predominant diffusing events with respect to ISRO (a) and BMRO (b), respectively. The type of events is indicated by the arrows, for example, "neighbor → outside" in (a) stands for events starting at ICO neighbor and ending outside ICO. Other types can be inferred similarly. The average time diffusing atoms have spent with respect to ICO and BMRO during t=0.6-1.8 μs were shown in (c) and (d), respectively.

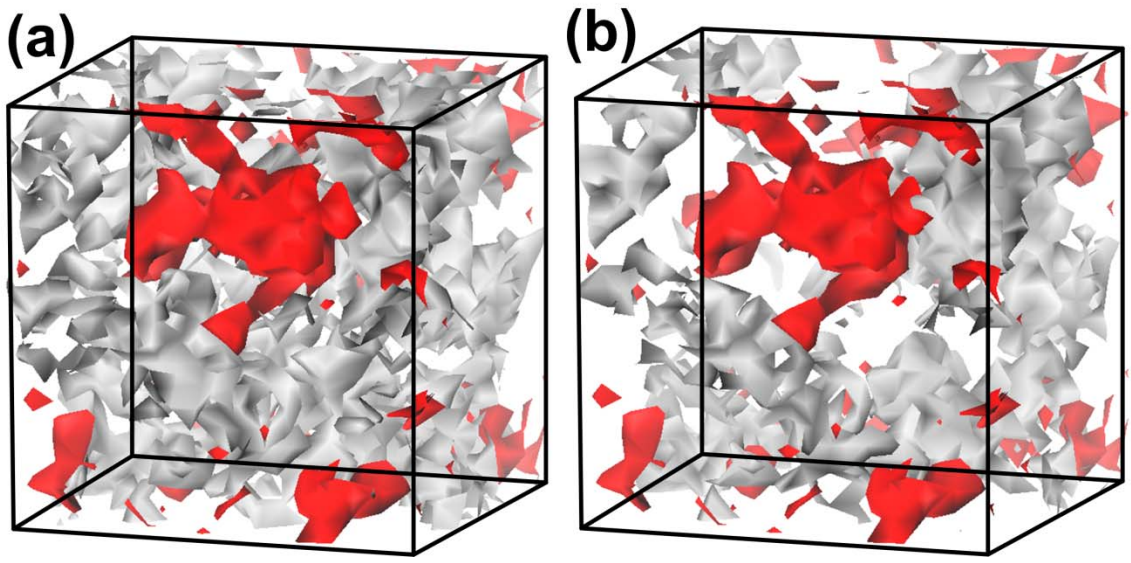

Fig. 3 (a) Spatial correlations of the diffusion paths with respect to ISRO (a) and the BMRO (b). The isosurface of the diffusion paths are colored in red, while the isosurface showing the time-averaged ISRO or BMRO is in gray.

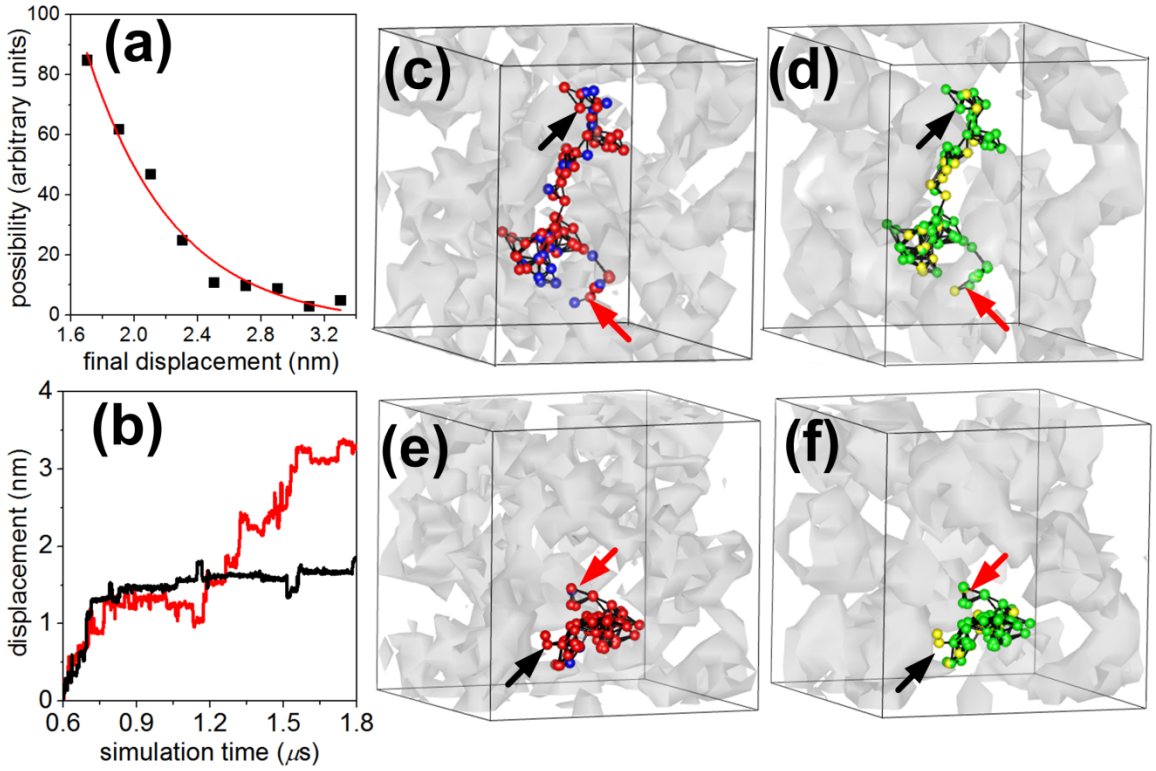

Fig. 4 (a) The distribution of final displacements at t=1.8 μs for the diffusing atoms. The solid line indicates fitting using an exponential decay function. (b) The time-dependent displacements of two representative diffusing atoms with the largest (in red) and smallest (in black) displacement at t=1.8 μs. The corresponding trajectories of the two diffusing atoms with respect to ISRO are shown in (c) and (e), respectively. Instantaneous atomic positions are colored in blue or red when the diffusing atom is an ICO neighbor or outside ICO, respectively. The same trajectories with respect to BMRO are shown in (d) and (f), respectively. Instantaneous atomic positions are colored in red or green when the diffusing atom is in the outer shell or outside the BMRO, respectively. The starting and end points of the trajectory are marked by the black and red arrows, respectively. All the atoms shown in this figure are Cu atoms.